

Quantum solitons in the sawtooth lattice

D. Sen and B. S. Shastry

Indian Institute of Science, Bangalore 560012, India

R. E. Walstedt and R. Cava

AT&T Bell Laboratories, Murray Hill, New Jersey 07974

(Received 13 September 1995)

We study the sawtooth lattice of a coupled spin 1/2 Heisenberg system, a variant of the railroad-trestle lattice. The ground state of this system is twofold degenerate with periodic boundary conditions and supports kink-antikink excitations, which are distinct in this case, unlike the railroad-trestle lattice. The resulting low-temperature thermodynamics is compared with the recently discovered delafossites $\text{YCuO}_{2.5}$.

I. INTRODUCTION

Several quantum topological excitations have been explored in the quantum antiferromagnetic spin systems in the past decade, expanding on the Anderson-Kubo spin waves. These include "spinons," i.e., spin 1/2 objects of Faddeev and Takhtajan,¹ a name coined by Anderson, describing the excitations of the isotropic one-dimensional Heisenberg spin 1/2 antiferromagnet (AFM), with a concomitant two-parameter elementary excitation spectrum with an asymptotic fourfold degeneracy. The anisotropic Heisenberg AFM in the Néel ordered, massive phase contains "domain walls" found by Johnson, Krinsky and McCoy² from Baxter's solution of the XYZ model. These domain walls separate two regions of Ising like ordered states, and propagate as dressed fermions³ (again these exhibit a fourfold degeneracy). The domain walls would broaden out and indeed the width would diverge with the correlation length as the isotropic point is reached, so the limiting excitation would have a delocalized character. It may be tempting to view the "spinons" as limiting cases of the domain walls, although the AFM order vanishes at the isotropic point. Yet another class of excitations were introduced by Shastry and Sutherland (SS) Ref. 4 in the context of models with broken translation symmetry.⁵ These are topological quantum solitons separating two regions of broken translational symmetry and have again a fourfold degeneracy of two-parameter excitations. In addition, these are fairly compact objects with a width consisting of a few lattice constants. In view of the theoretical interest in these constructs, it is interesting to ask for experimental realizations of such systems.

Recently a family of delafossite compounds have been synthesized which seem to be promising from this viewpoint. The YCuO_2 lattice consists of planes of coupled Y_2O_4 octahedra linked by twofold-coordinated bridging Cu^+ ions, which form a triangular planar array. It is possible to intercalate O^{2-} ions into the Cu^+ planes, forming different lattice symmetries depending on the amount of intercalant. For compositions up to and including $\text{YCuO}_{2.5}$, the planar O^{2-} form an orthorhombic structure.⁶ At the upper limit of this range one has a magnetic insulator, with all of the copper ions converted to Cu^{2+} . For compositions with additional oxygen beyond $\text{O}_{2.5}$, the structural symmetry becomes hex-

agonal and mobile hole carriers appear, rendering the CuO_x planes weakly conducting.⁷

Preliminary data on the structure of the orthorhombic phase for $\text{YCuO}_{2.5}$ suggests two sets of locally triangular configuration of copper sites with O^{2-} ions in the center of one of the sets of triangles, providing superexchange paths (Fig. 1). The two sets of triangles are separated and have no O^{2-} ions in their midst, so we have a good possibility of one-dimensional exchange coupled Cu^{2+} , i.e., a $S=1/2$ system. We have carried out NMR measurements of the rates $1/T_1, 1/T_2$ of ^{63}Cu between 70 K and 230 K. It is evident from the NMR results that there are substantial exchange couplings between the $S=1/2$ Cu^{2+} spin moments in this structure. The asymptotic low-temperature behavior of T_1 is activated with an activation energy of ~ 650 K. Such couplings would arise between nearest neighbor spins to an O^{2-} ion, which would act as the conduit for 120° exchange paths. If we presume that such couplings between nearest neighbor and second-neighbor spins to an O^{2-} ion are negligible (60° exchange paths), then the system divides into a series of parallel one-dimensional "sawtooth" lattices of exchange coupled spins, which are only weakly interacting. Such a system, the sawtooth lattice is analyzed in this paper, and shown to have an interesting and unique set of magnetic excitations, namely quantum solitons very similar to the ones discussed in SS, with a notable feature, namely the kink-antikink symmetry in the Majumdar model is broken here.

II. THE SAWTOOTH CHAIN: ANALYTICAL RESULTS

The Hamiltonian for the sawtooth chain may be written as a sum of Hamiltonians governing triangles of spins (see Fig. 2)

$$H = \sum_{n=1}^N H_n, \quad (2.1)$$

$$H_n = \frac{J}{2} \left[(\vec{S}_{2n-1} + \vec{S}_{2n} + \vec{S}_{2n+1})^2 - \frac{3}{4} \right].$$

Here N is the number of triangles and J denotes the antiferromagnetic coupling. We may consider either open chains (with $2N+1$ sites) or periodic chains (with $2N$ sites).

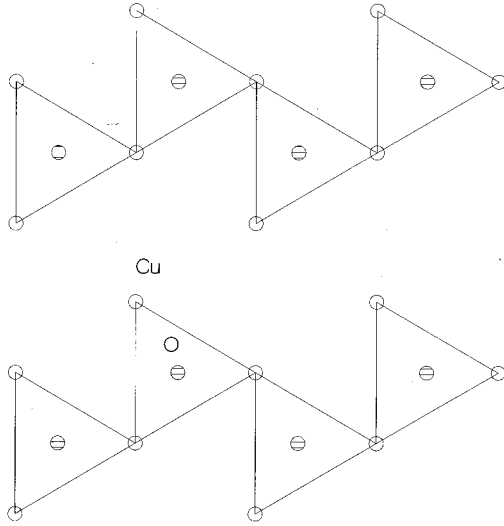


FIG. 1. A picture of the CuO planes in YCuO_{2.5} from preliminary structural data.

To find the ground states of (2.1), we note that H_n is proportional to a projection operator since its eigenvalues are 0 (if the total spin in triangle n is $1/2$) and $3J/2$ (if the total spin is $3/2$). For two sites i and j with $i < j$, we denote the singlet state mathematically by $[i, j] = (|\alpha_i \beta_j\rangle - |\beta_i \alpha_j\rangle) / \sqrt{2}$, and pictorially by a double line joining i and j as indicated in Figs. 3 and 4. (Here α_i and β_i denote spin up and down respectively at site i .) Then the states with total spin $1/2$ in triangle n can be thought of as either $[2n-1, 2n]$ with the spin at site $2n+1$ free (either α or β), or as $[2n, 2n+1]$ with the spin at $2n-1$ free. The other possible pairing $[2n-1, 2n+1]$ is linearly dependent since

$$[2n, 2n+1] \alpha_{2n} = [2n-1, 2n] \alpha_{2n+1} + [2n, 2n+1] \alpha_{2n-1}. \tag{2.2}$$

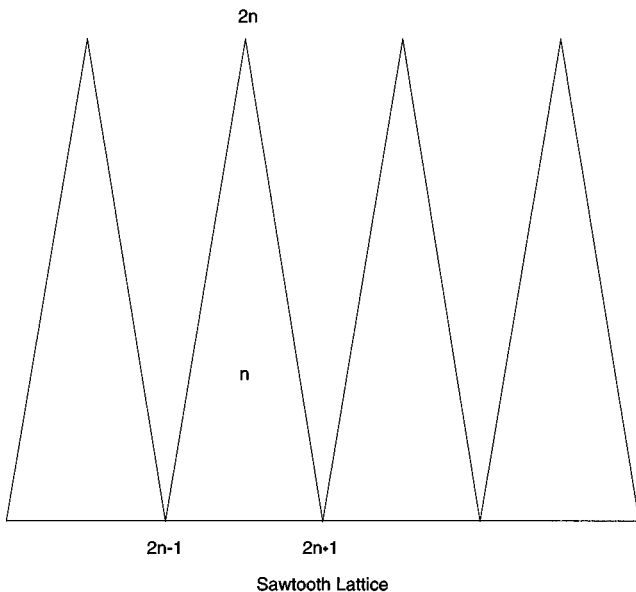


FIG. 2. The sawtooth chain. The three sites forming triangle n are numbered as shown.

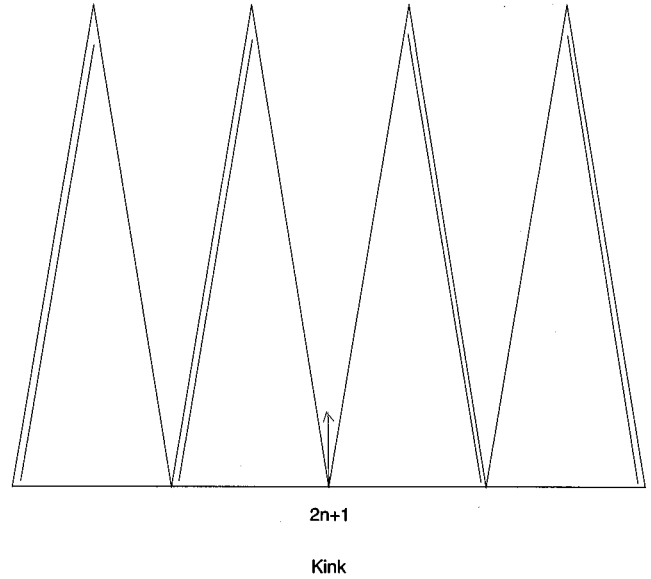


FIG. 3. A kink configuration with the free spin at site $2n+1$. The double lines indicate singlets.

It is now easy to show that the periodic chain has two degenerate ground states (with energy $E_o=0$) given by

$$|I\rangle = \prod_{n=1}^N [2n-1, 2n] \tag{2.3}$$

and

$$|II\rangle = \prod_{n=1}^N [2n, 2n+1],$$

where $\vec{S}_{2N+1} \equiv \vec{S}_1$.^{4,8} The open chain has $2(N+1)$ degenerate ground states (with $E_o=0$) given by

$$|2n+1, \alpha \text{ or } \beta\rangle = \left(\prod_{n=1}^m [2n-1, 2n] \right) \times \left(\prod_{n=m+1}^N [2n, 2n+1] \right) \times \alpha_{2m+1} \text{ or } \beta_{2m+1}, \tag{2.4}$$

where m may take any value from 0 to N . Such a state is shown in Fig. 3. This configuration can be thought of as a kink at site $2m+1$ which separates the ground state I on its left from the ground state II on its right. Since all states in (2.4) have the same energy (namely, zero), a linear combination of them like

$$|k\rangle = \frac{1}{\sqrt{N}} \sum_{m=0}^N \exp(ikm) |2m+1, \alpha\rangle \tag{2.5}$$

has the same energy for all values of k . In the limit $N \rightarrow \infty$, (2.5) denotes a momentum eigenstate. We therefore see that kinks in the sawtooth chain have the dispersionless spectrum $\omega(k)=0$. Further, kinks only differ from ground states I and II at a single site.

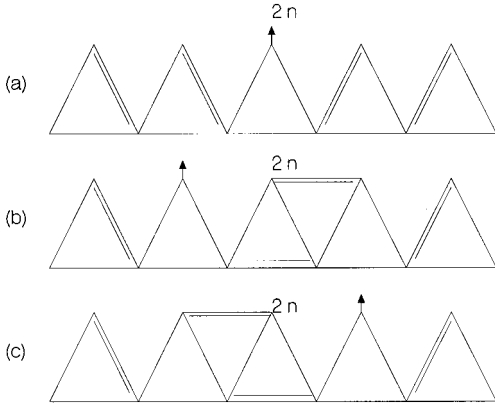


FIG. 4. The three antikink configurations centered about site $2n$. (a) is a 1 cluster while (b) and (c) are 5 clusters.

We will see below that *antikinks* are quite different in that they have a nontrivial dispersion and they do not just differ from the states I and II at only one site. In fact, we are unable to solve for the wave function and dispersion of antikinks exactly. The best we can do is to variationally estimate these quantities more and more accurately by considering antikink configurations spread over 1 site, 5, sites and so on.

We would like to make a few comments before examining the antikinks. First, it can be shown by induction that the states in (2.3) and (2.4) are indeed the only ground states for the sawtooth chain.⁹ Secondly, it can be proved rigorously that there is a finite gap between the ground states and the first excited state.^{10,11} Our discussion of antikinks will lead to an accurate estimate of this gap. Finally, the situation here may be contrasted with that obtaining in the railroad trestle which was first studied by Majumdar and co-workers.⁵ The Hamiltonian for the railroad trestle differs from (1) in also having a H_n for the sites $(2n, 2n+1, 2n+2)$. As a result, this model only has the two ground states of types I and II (except possibly for free spins at the ends if the chain is open). There is a finite gap to excited states. Kinks and antikinks are on the same footing in the railroad trestle. They are not exactly solvable but they can be shown to have identical dispersions.

We now study antikinks to a first approximation by considering a state like the one shown in Fig. 4(a). This is a configuration which has ground state II to the left of a 1-site cluster (located at site $2n$) and ground state I to its right. We denote this state by $|2n\rangle_1$. (For simplicity of notation, we will henceforth drop the spin index, α or β , of the free spin.) In the limit $N \rightarrow \infty$, we consider a momentum eigenstate

$$|k\rangle = \frac{1}{\sqrt{N}} \sum_n \exp(ikn) |2n\rangle_1. \quad (2.6)$$

This state has a nontrivial norm because

$${}_1\langle 2n|2m\rangle_1 = (-1)^{n-m} 2^{|n-m|}. \quad (2.7)$$

Hence

$$\langle k|k\rangle = 3/(5 + 4 \cos k). \quad (2.8)$$

Further

$${}_1\langle 2n|H|2m\rangle_1 = \frac{3}{4} J \delta_{nl} \delta_{lm} \quad (2.9)$$

implies that

$$\langle k|H|k\rangle = \frac{3}{4} J. \quad (2.10)$$

Our estimate of the dispersion based on this 1-cluster calculation is therefore

$$\omega(k) = \left(\frac{5}{4} + \cos k \right) J. \quad (2.11)$$

[The kinks and antikinks in the railroad trestle have the same dispersion as in (2.11) for the 1-cluster approximation.] Equation (2.11) has a minimum at $k = \pi$ where the antikink energy is $J/4$. This is our first estimate of the gap in the open chain and, as we will argue below, in the periodic chain also.

We may now improve our estimate by considering 3-cluster configurations. Due to Eq. (2.2), however, a cluster of three neighboring sites with $S=1/2$ can be reduced to a superposition of 1-cluster states like $|2n\rangle_1$. So we have to continue on to 5-cluster configurations. The only two linearly independent configurations that we need to consider are the ones shown in Figs. 4(b) and 4(c). We denote these two by $|2n\rangle_2$ and $|2n\rangle_3$ respectively where $2n$ denotes the center of the 5 clusters. Note that $|2n\rangle_2$ and $|2n\rangle_3$ are related to each other by reflection about the site $2n$. We now consider a momentum eigenstate with two complex variational parameters a and b

$$|k, a, b\rangle = \frac{1}{\sqrt{N}} \sum_n \exp(ikn) [|2n\rangle_1 + a |2n\rangle_2 + b |2n\rangle_3], \quad (2.12)$$

and minimize $\omega(k, a, b)$ by varying a and b . The computation is straightforward though lengthy. We first obtain the overlaps

$$\begin{aligned} {}_2\langle 2n|2m\rangle_1 &= -(-1)^{n-m} 2^{|n-m|} \text{ if } n \geq m+1, \\ &= -1/4 \text{ if } n=m, \end{aligned} \quad (2.13)$$

$$= \frac{1}{2} (-1)^{n-m} 2^{|n-m|} \text{ if } n \leq m-1,$$

$$\begin{aligned} {}_2\langle 2n|2m\rangle_2 &= 1 \text{ if } n=m, \\ &= -1/8 \text{ if } |n-m|=1, \end{aligned} \quad (2.14)$$

$$= -\frac{1}{2} (-1)^{n-m} 2^{|n-m|} \text{ if } |n-m| \geq 2,$$

$$\begin{aligned}
{}_2\langle 2n|2m\rangle_3 &= (-1)^{n-m}/2^{|n-m|} \text{ if } n \geq m+2, \\
&= -1/8 \text{ if } n=m+1, \\
&= -1/2 \text{ if } n=m, \\
&= 1/4 \text{ if } n=m-1, \\
&= \frac{1}{4}(-1)^{n-m}/2^{|n-m|} \text{ if } n \leq m-2.
\end{aligned} \tag{2.15}$$

All other overlaps can be obtained by using the reflection symmetry mentioned above. Thus

$${}_3\langle 2n|2m\rangle_1 = {}_2\langle 2m|2n\rangle_1, \tag{2.16}$$

and

$${}_3\langle 2n|2m\rangle_3 = {}_2\langle 2n|2m\rangle_2,$$

We therefore obtain

$$\begin{aligned}
\langle k|k\rangle &= \frac{1}{5+4 \cos k} [(5+4 \cos k)A_1 + (4+2e^{-ik})A_2 \\
&\quad + (4+2e^{ik})A_2^*],
\end{aligned}$$

where

$$\begin{aligned}
A_1 &= 1 - \frac{1}{4}(a+a^*+b+b^*) + \frac{1}{4}(aa^*+bb^*)(4-\cos k) \\
&\quad - \frac{1}{2}(ab^*+ba^*) + \frac{1}{8}ab^*(2e^{-ik}-e^{ik}) \\
&\quad + \frac{1}{8}ba^*(2e^{ik}-e^{-ik}),
\end{aligned}$$

and

$$\begin{aligned}
A_2 &= \frac{e^{ik}}{4}(-2-a^*+2a-b+2b^*) \\
&\quad + \frac{e^{i2k}}{16}(-2aa^*-2bb^*+4ab^*+ba^*). \tag{2.17}
\end{aligned}$$

Next we calculate the matrix elements of H_n . Thus

$$\begin{aligned}
{}_2\langle 2n-2|H_n|2n\rangle_1 &= -\frac{3}{8}J, \\
{}_2\langle 2n+2|H_n|2n\rangle_1 &= \frac{3}{8}J, \\
{}_2\langle 2n-4|H_{n-1}|2n\rangle_2 &= -\frac{3}{16}J, \\
{}_2\langle 2n|H_{n-1}|2n\rangle_2 &= \frac{3}{4}J, \\
{}_3\langle 2n-4|H_{n-1}|2n\rangle_2 &= \frac{3}{16}J,
\end{aligned} \tag{2.18}$$

$${}_3\langle 2n|H_{n-1}|2n\rangle_2 = -\frac{3}{8}J,$$

$${}_2\langle 2n-4|H_{n-1}|2n\rangle_3 = \frac{3}{16}J.$$

All other matrix elements can either be obtained from the above by translation or reflection symmetry, or are zero. We then find that

$$\begin{aligned}
\langle k|H|k\rangle &= \frac{3}{4} + i\frac{3}{4} \operatorname{sinc}(a-a^*-b+b^*) + \left(\frac{3}{2} - \frac{3}{8} \cos 2k\right) \\
&\quad \times (aa^*+bb^*) + \left(\frac{3}{8} \cos 2k - \frac{3}{4}\right)(ab^*+ba^*).
\end{aligned} \tag{2.19}$$

We have found that the minimum value of $\omega(k)$ occurs at $k=\pi$ if we take $a=b$ to be real. Then

$$\omega(\pi; a) = \frac{1}{4} \frac{1+2a^2}{1-a+a^2/2}. \tag{2.20}$$

This has a minimum at $a=(3-\sqrt{17})/4=-0.2808$ where $\omega=0.2192J$. [For the railroad trestle, $\langle k|k\rangle$ is the same as in (2.17) while $\langle k|H|k\rangle$ has the extra term $3(aa^*+bb^*)/4$ on the right hand side of (2.19). Hence

$$\omega(\pi; a) = \frac{1}{4} \frac{1+4a^2}{1-a+a^2/2}, \tag{2.21}$$

whose minimum value is 0.2344J.]

We see that the estimate of the gap changes relatively little on going from 1 cluster to 5 clusters. This is because of the small correlation length ξ in this system. We expect that the estimate of the gap $\Delta(l)$ from an l -cluster calculation will differ from the true gap $\Delta(\infty)$ by terms of order $\exp(-l/\xi)$. The gap in the railroad trestle chain has been estimated from a 9-cluster calculation in Ref. 12. From the values $\Delta(1)=0.25J$, $\Delta(5)=0.2344J$, and $\Delta(9)=0.2340J$, we estimate that $\xi \sim 1.1$. While we have not computed $\Delta(9)$ for the sawtooth chain, we expect that it will differ very little from $\Delta(5)$ for a similar reason.

To summarize so far, we have seen that kinks have zero dispersion while antikinks have a dispersion with a gap of 0.2192J at $k=\pi$. We now identify the latter figure with the gap in the open chain. This assumes that there are no bound states of several kinks and antikinks which have a lower energy. For the railroad trestle, it is in fact known that there is no bound state of a kink and an antikink which has lower energy than a well-separated kink and antikink.⁴

We will now argue that a periodic chain has the same gap and, further, that it has a dispersionless spectrum for its lowest excitation. Any excitation in a periodic chain must consist of a succession of alternating kinks and antikinks. In the absence of low-energy bound states, the lowest excitation in a long periodic chain will consist of one kink well separated from one antikink. The energy of this state is the sum

$$\omega(Q) = \omega_K(k_1) + \omega_{\bar{K}}(k_2), \tag{2.22}$$

where k_1 and k_2 denote the momenta of the kink (K) and the antikink (\bar{K}), and the total momentum of this state is $Q = k_1 + k_2$. It is now clear that since $\omega_K(k_1) = 0$ for all k_1 , the minimum possible value of $\omega(Q)$ is given by the constant $\Delta \equiv \omega_{\bar{K}}(\pi)$ since we can always choose $k_1 = Q - \pi$.

Indeed, numerical studies of finite periodic chains up to $N = 10$ by Kubo had indicated the existence of a dispersionless spectrum with $\omega(Q) \approx 0.219J$ for all Q .¹³ We now have the explanation of this striking property of the periodic sawtooth as arising from the dispersionless spectrum of the kink. Further, our 5-cluster computation has already yielded an estimate of the gap which is very close to the value obtained numerically.

We may now use the above results to study low-temperature thermodynamic properties of the sawtooth chain. For instance, we can estimate the magnetic susceptibility based on the picture of a low density of alternating kinks and antikinks which are well separated and noninteracting. In the presence of an external magnetic field B , they have the energies $-2\mu S_z$ and $\omega_{\bar{K}}(k) - 2\mu S_z$ respectively where μ is the Bohr magneton. If we use the 1-cluster expression for $\omega_{\bar{K}}(k)$ given in Eq. (11), we obtain the partition functions for one kink and one antikink as

$$x_K = 2 \cosh(\mu\beta B) \quad (2.23)$$

and

$$x_{\bar{K}} = 2 \cosh(\mu\beta B) I_o(\beta J) \exp\left(-\frac{5}{4}\beta J\right),$$

respectively, where $\beta = 1/k_B T$ is the inverse temperature and I_o is a modified Bessel function. The free energy per site is then given by

$$f = -\frac{1}{\beta} (x_K x_{\bar{K}})^{1/2}, \quad (2.24)$$

and the magnetic susceptibility per site $\chi = -(\partial^2 f / \partial B^2)_{B=0}$ is

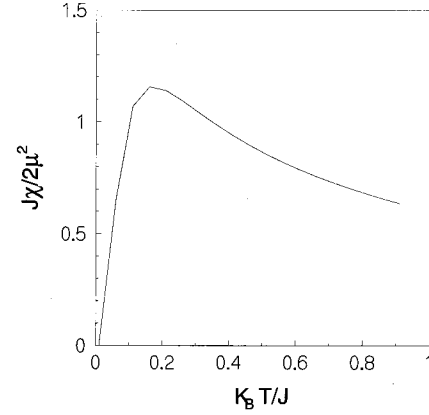


FIG. 5. Low-temperature magnetic susceptibility as a function of $k_B T/J$.

$$\frac{J\chi}{2\mu^2} = \beta J \left[I_o(\beta J) \exp\left(-\frac{5}{4}\beta J\right) \right]^{1/2}. \quad (2.25)$$

Note that this thermodynamic quantity exhibits a gap equal to $J/8$ at very low temperature which is half the sum of the gaps for the kink (zero) and the antikink ($J/4$). In Fig. 5, we show the magnetic susceptibility as a function of $k_B T/J$.

Coming back to the system $\text{YCuO}_{2.5}$, we see that the gap of $\sim 0.22J$, if equated to the NMR activation energy, implies that $J \sim 3000$ K, which is rather too large. Indeed, the largest J 's are a factor of 2 smaller than this, as measured in the high- T_c systems, which have comparable Cu-O bond lengths as in these compounds, namely ~ 2 Å. It then seems likely that these systems either do not allow for a decoupling between these sawtooth lattices, forcing say a pair of these excitations, or else there might be pairwise dimerization, which could be signalled in detailed structural studies. It would be interesting to study these issues in detail experimentally, as would the ESR on these systems at elevated temperatures, say 700 K, where the fourfold degeneracy would be reflected in the existence of free spin 1/2 excitations with a thermally activated density.

We recently became aware of a paper by T. Nakamura and K. Kubo,¹⁴ dealing with the excitations of the same lattice.

¹L. Faddeev and L. Takhtajan, Phys. Lett. **85A**, 375 (1981).

²J. D. Johnson, B. McCoy, and S. Krinsky, Phys. Rev. A **8**, 2526 (1973).

³G. Gomez-Santos, Phys. Rev. B **41**, 6788 (1990).

⁴B. S. Shastri and B. Sutherland, Phys. Rev. Lett. **47**, 964 (1981).

⁵C. K. Majumdar, J. Phys. C **3**, 911 (1969); C. K. Majumdar and D. K. Ghosh, J. Math. Phys. **10**, 1388 (1969); **10**, 1399 (1969); C. K. Majumdar, K. Krishan, and V. Mubayi, J. Phys. C **5**, 2896 (1972).

⁶R. J. Cava *et al.*, J. Solid State Chem. **104**, 437 (1993); R. J. Cava, W. F. Peck, Jr., J. J. Krajewski, S-W. Cheong, and H. Y. Hwang, J. Mater. Res. **9**, 314 (1994).

⁷R. E. Walstedt *et al.*, Phys. Rev. B **49**, 12 369 (1994).

⁸M. W. Long and R. Fehrenbacher, J. Phys. Condens. Matter **2**, 2787 (1990).

⁹F. Monti and A. Sütö, Phys. Lett. A **156**, 197 (1991).

¹⁰I. Affleck, T. Kennedy, E. H. Lieb, and H. Tasaki, Commun. Math. Phys. **115**, 477 (1988).

¹¹S. Knabe, J. Stat. Phys. **52**, 627 (1988).

¹²W. J. Caspers, K. M. Emmett, and W. Magnus, J. Phys. A **17**, 2687 (1984).

¹³K. Kubo, Phys. Rev. B **48**, 10 552 (1993).

¹⁴T. Nakamura and K. Kubo, preceding paper, Phys. Rev. B **53**, 6393 (1996).